International Journal of
Scientific Research in Science and Technology (IJSRST)
Print ISSN : 2395-6011, Online ISSN : 2395-602X
International Conference on Advanced Materials
Held on 14, 15 December 2017, Organized by Department of Physics,
St. Joseph's College, Trichy, Tamilnadu, India

Synthesis and Characterisation of Nickel Ferrite Nanoparticles Prepared by Spray Pyrolysis Method

Anila I[1], Subin P. John[1], Jacob Mathew M[1*]
[1]Department of Physics, Mossbauer Research Group, St. Berchmans College, Changanassery, India
*Corresponding Author email: jacob.chrisdale@gmail.com

Abstract

Nickel ferrite nanoparticles of ultrafine size were successfully prepared by spray pyrolysis method. The structural characterization of the samples is done using XRD and FTIR. XRD pattern of all samples show the formation of single phase cubic spinel structure.The distribution of cations among the two interstitial sites has been estimated by the Rietveld refinement of XRD pattern. The FTIR spectra show two strong absorption bands, confirm the presence of metal - oxygen complexes within the spinel lattice. The HRTEM micrographs demonstrates ultrafine particles having cubic morphology and the average particle size obtained is in good agreement with that estimated from XRD. The elemental analysis has been carried out using EDS, confirmed the purity of the synthesized sample. The room temperature magnetic properties of the sample were measured by using a VSM and revealed the soft magnetic nature of the sample and the same has been confirmed by room temperature Mossbauer studies. The cation distribution estimated from Mossbauer spectroscopy and Rietveld refinement confirm the mixed spinel structure of the spray pyrolysis synthesized Nickel ferrite nanoparticles.

Keywords: Nickel ferrite, spray pyrolysis method, nano ferrite, Rietveld refinement, Mossbauer studies.

1. Introduction

Studies on magnetic nanoparticles (MNPs) belonging to spinel ferrites is an active area of research due to their potential use in recording media, information storage and magneto-optical devices [1]. Most of these studies are focussed on the influence of various synthesis conditions, starting materials and size and shape etc on the magnetic nature of such nano systems using state of art analytical tools [2]. Recently many studies are being carried on the usefulness of spinel magnetic nano systems in biomedical applications [3]. Nickel ferrite nano systems is one of the important groups of particles that has potential applications in biomedical field, especially in hyperthermia applications [3]. They are less toxic and chemically stable, compared to pure nickel, and appears to be a viable alternative for pure nickel in biomedical applications. In the present work, we have tried to synthesis nickel ferrite nanoparticles by spray pyrolysis of eco-friendly polymer precursor -polyvinyl alcohol (PVA). We have synthesized nickel ferrite nanosystems using a low-cost spray pyrolysis unit in which polymer precursor-mixture of metal nitrates and PVA dissolved in de-ionised water-sprayed over a hot glass plate kept at fixed temperature.

2. Material and methods

Nickel ferrites nanoparticles were synthesized by spray pyrolysis method. All the reagents used for the synthesis of nickel ferrite nanoparticles were analytical grade. The stoichiometric amounts of nickel nitrate ($Ni(NO_3)_2.6H_2O$) and ferric nitrate ($Fe(NO_3)_3.9H_2O$) were dissolved in deionized water

International Journal of
Scientific Research in Science and Technology (IJSRST)
Print ISSN : 2395-6011, Online ISSN : 2395-602X
International Conference on Advanced Materials
Held on 14, 15 December 2017, Organized by Department of Physics,
St. Joseph's College, Trichy, Tamilnadu, India

under magnetic stirring. The raw materials were mixed with aqueous solution of PVA. The resulting viscous solution of PVA metal nitrates is sprayed on a glass plate in the spray pyrolysis unit. The glass substrate slowly cooled and peal out sample from the substrate. The sample is annealed at 450,500,550,600^{0}C to obtain the single-phase spinel nickel ferrite nanoparticles and is named as NP1-NP4.

The crystallinity, phase structure and nano-behavior of the samples were characterized by X-ray diffraction (XRD). One of the samples is selected for further characterisation studies like High ResolutionTransmission electron microscopy (HRTEM), Fourier transform infrared spectroscopy (FT-IR), Energy dispersive electron spectroscopy (EDS), vibrating sample magnetometer (VSM) and Mossbauer techniques.

3. Results and Discussion

3.1. X-ray diffraction (XRD) analysis

X-ray patterns of samples are shown in Figure 1. The dominant peaks observed at 2θ = 30.298^0, 35.69^0, 37.48^0, 43.38^0, 53.99^0, 57.38^0, 63.02^0 and 75.45^0 corresponds to (220), (311), (222), (400), (422), (511), (440) and (533) planes of $NiFe_2O_4$ agrees well with a cubic spinel structure (JCPDS PDF card No: # 86-2267, $Fd\bar{3}m$ space group). The patterns confirm the formation of single phase cubic spinel ultrafine nickel ferrite nanoparticles. The broadening of diffraction peaks indicates samples are in nano regime. As the annealing temperature increases the intensity of diffraction peaks increases, especially for (311) peak, demonstrating the improvement of crystallinity of the sample. The average crystallite size of the nano crystallite sample is determined from the full width at half maximum (FWHM) of the XRD patterns using Scherrer's equation.

$$\text{Dhkl} = \frac{0.9\lambda}{\beta\cos\theta} \qquad (1)$$

where, 'D_{hkl}' is thecrystallite size, 'λ' is the wave length of the used X-ray (λ = 0.15406nm), 'β' is the full width at half maximum (FWHM) in radian and 'θ' is the half diffraction angle in degree. The average crystallite sizes have been estimated and found to increase with the increasing annealing temperature. This may be due to the coalescence of the particles by solid-state diffusion where the system reduces its free energy by reducing the surface area of the nanoparticles [4]. The lattice parameter 'a' of the samples were calculated by using the Bragg's equation,

$$\text{a} = d\sqrt{h^2+k^2+l^2} \qquad (2)$$

where 'h', 'k', 'l' are the Miller indices of the crystal planes and 'd' is the inter planer spacing.

The X-ray density of the samples are calculated using the formula,

$$\rho_x = \frac{8M}{Na^3} \qquad (3)$$

where 8 is the number of molecules per unit cell of spinel lattice, 'M' is the molecular weight, 'N' is Avogadro's number and 'a' is the lattice parameter. The average crystallite size, lattice parameter, and X-ray density of all the samples are calculated and the value obtained for NP3 is in good agreement with the reported value of 8.33 Å (Table1) [2]. The increases of lattice constant values from 8.32 to 8.34 Å with the temperature is because of the expansion of the particle volume with temperature. Thelattice parameter and crystallite size growth as functions of temperature are plotted in Figure 2.

International Journal of
Scientific Research in Science and Technology (IJSRST)
Print ISSN : 2395-6011, Online ISSN : 2395-602X
International Conference on Advanced Materials
Held on 14, 15 December 2017, Organized by Department of Physics,
St. Joseph's College, Trichy, Tamilnadu, India

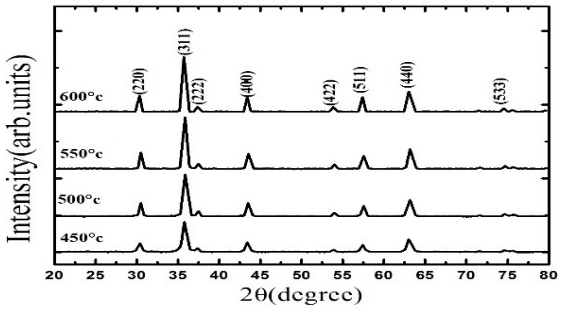

Figure 1. XRD patterns of $NiFe_2O_4$ nanoparticle annealed at different temperatures

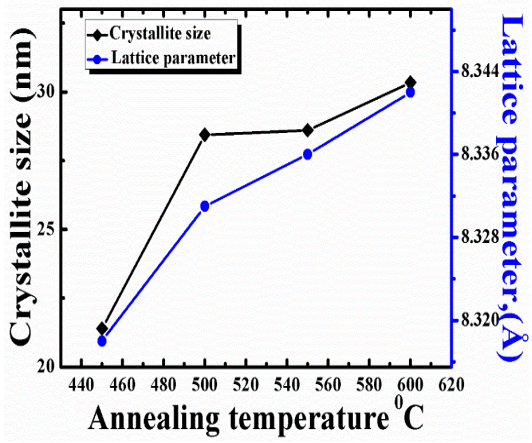

Figure 2. The lattice parameter and crystallite size growth as functions of annealing temperature

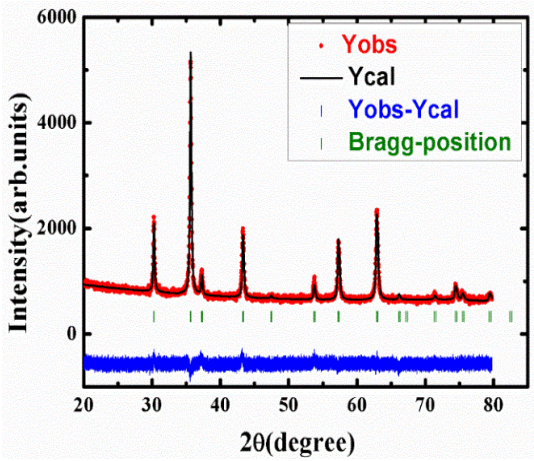

Figure 3. Rietveld refined x-ray diffraction pattern of the sample NP3

The lattice constant calculated for sample NP3 matches well with values reported in literature [2] and therefore selected for further characterisation studies using advanced techniques. The accurate knowledge of cation distribution over the crystallographic sites is significant in the determination of the physical properties of the synthesized sample. It can be estimated from the Rietveld refinement of X-ray diffraction pattern by using Full-Prof programme and the refined pattern of the sample NP3 is shown in Figure 3. Here, the red dots represent the experimental data, and calculated intensities are shown as black solid line. The bottom blue line represents the difference between the measured and the calculated intensities. The allowed Braggs positions for $Fd\bar{3}m$ space group are marked as verticallines. The pattern confirms the formation of single phase cubic spinel structure without any signature of secondary phase. The refined parameters of sample NP3 are summarized in Table 1. The lattice parameter obtained from the Rietveld refinement is perfectly matches with the experimental results obtained from XRD pattern (table 1). The R_p factor is found to be large [5]. It could be due to the low signal to noise ratio of XRD patterns for nanocrystalline materials. However, the low value of χ^2 justifies the goodness of refinement. The estimated cation distribution from the Rietveld analysis for sample NP3 is given in Table 1, which reveals that the sample have mixed spinel structure.

Table 1. Parameters estimated from XRD of $NiFe_2O_4$ nanoparticle annealed at different temperatures andRietveld refinement parameters & Cation distribution of the sample NP3

International Journal of
Scientific Research in Science and Technology (IJSRST)
Print ISSN : 2395-6011, Online ISSN : 2395-602X
International Conference on Advanced Materials
Held on 14, 15 December 2017, Organized by Department of Physics,
St. Joseph's College, Trichy, Tamilnadu, India

Sample code	Crystallite size from XRD, D_{XRD} (nm)	Lattice parameter, a (Å)	X-ray density (gm/cm^3)	Crystal system	Space group	R_p	χ^2	a = b = c (Å)	Cation distribution
NP1	21.40	8.318	5.39	-	-	-	-	-	-
NP2	28.44	8.331	5.42	-	-	-	-	-	-
NP3	28.61	8.336	5.43	Cubic	$Fd\bar{3}m$	33.8	1.36	8.335	$(Ni_{0.11}Fe_{0.89})A$ $[Ni_{0.89}Fe_{1.11}]^B O_4$
NP4	30.34	8.342	5.38	-	-	-	-	-	-

3.2. HRTEM studies

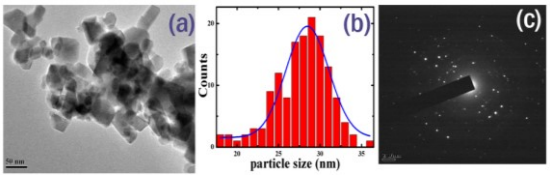

Figure 4. (a) HRTEM image, (b) particle size distribution and (c) SAED pattern of the sample NP3

The morphology and particle size distribution of the sample NP3 is investigated by using HRTEM. HRTEM micrographs demonstrates ultrafine particles having cubic morphology and average particle size obtained from HRTEM is 28.49 nm which is in good agreement with particle sizes estimated from XRD. The broken rings in the SAED pattern reveal polycrystalline nature of the sample. The particle sizedistribution can be well fitted to lognormal distribution and is given in figure 4.

3.3. FTIR Analysis

FTIR spectra of the sample NP3 is shown in the figure 5. The spectra show two main absorption bands v_1 and v_2 in the range of 400 cm^{-1} to 1000 cm^{-1} as a common feature of all spinel structures. The higher band, v_1 observed around in the frequency range 550-600 cm^{-1} is attributed to the intrinsic metal oxygen stretching vibrations at the tetrahedral site whereas, the v_2 lowest band is usually observed around in the frequency range 450-500 cm^{-1}, is assigned to octahedral metal oxygen stretching vibrations [6], which confirms the formation of spinel cubic ferrites nanoparticles. There are two bands at 551 and 594 cm^{-1} (v_1). These are the sub-bands of tetrahedral A-site. The splitting of tetrahedral band shows that some of the Ni^{+2}ions are shifted from octahedral site to tetrahedral site [7]. The cation distribution deduced from the Rietveld refinement of the sample NP3 confirm some fraction Ni^{+2} ions present in the tetrahedral sites (A-sites). Accordingly, the weak band at v_1 = 594 cm^{-1} could be attributed to the vibration of Ni^{2+} - O^{2-} in tetrahedral sites. FTIR spectra confirm the inverse spinel structure of the synthesized sample.

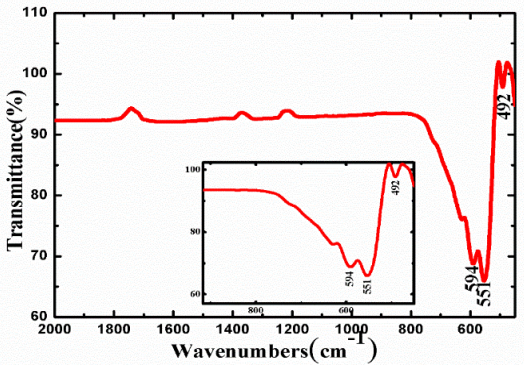

Figure 5. FT-IR spectrum of the sample NP3

3.4. EDS Analysis

The Energy Dispersive X-ray Spectroscopy analysis (EDS) was done to determine the chemical composition of the sample and confirmed stoichiometry of the investigated sample. EDS patterns of the sample is shown in figure 6 and the

International Journal of
Scientific Research in Science and Technology (IJSRST)
Print ISSN : 2395-6011, Online ISSN : 2395-602X
International Conference on Advanced Materials
Held on 14, 15 December 2017, Organized by Department of Physics,
St. Joseph's College, Trichy, Tamilnadu, India

atomic weight percentage of various cations in the investigated sample is given in table 2. There is no trace of any impurity was found which indicates purity of the sample.

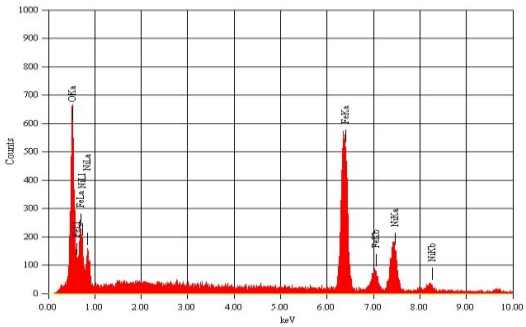

Figure 6. EDS spectrum of sample NP3

Table 2. Parameters obtained from of EDS spectrum of sample NP3

Element	(keV)	Mass%	Atom%	K
O K	0.525	36.79	67.35	46.31
Fe K	6.398	43.55	22.84	32.71
Ni K	7.471	19.67	9.81	13.58
Total		100	100	

3.5. Magnetic Studies

The room-temperature magnetization measurement of the sample up to maximum applied field of ± 15kOe is performed using a vibrating sample magnetometer (VSM). Hysteresis curve (M-H) curve of the sample is shown in the figure 7. The various magnetic properties like saturation magnetization (M_s), remanent magnetization (M_R), squareness ratio (S) and coercivity (H_c) are estimated from the M-H curve. The M-H curve with small value of coercivity reflects soft ferrimagnetic nature of the sample. The parameters obtained from hysteresis curve are listed in the Table 3.

The saturation maximum magnetization of the sample was found to be 42.35 emu/g, which is about 15% smaller than the saturation magnetization of 50 emu/g of bulk $NiFe_2O_4$ samples [8]. This reduced value of saturation magnetization with grain size reduction is explained in terms of the core shell structure of magnetic nanoparticles having spin glass like magnetically dead surface layer, where a ferrimagnetic core is surrounded by a surface layer of canted spins (existence of random canting of particle surface spins). According to Chen et al. [9], the thickness of dead layer is deduced from the equation

$$t = \frac{D}{6}\left(1 - \frac{M_s(nano)}{M_s(bulk)}\right) \qquad (4)$$

Here 'D' is the particle size obtained from lognormal distribution of HRTEM, M_s(nano) saturation of magnetization values of the samples, and the values of the M_s(bulk) were taken from Maensiri et al. [8]. The estimated value of the dead layer thickness 't' is listed in the table 3. The existence of the nonmagnetic dead layer might be caused by the canting of the surface spins or loss of the long-range order in the surface layer.

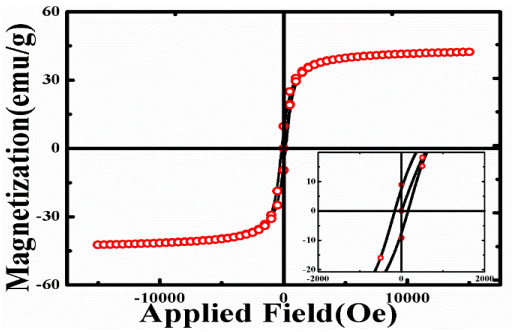

Figure 7. Room temperature magnetic hysteresis of the sample NP3 and portion near the origin is given in insight

Table 3. Magnetic parameters obtained from M-H curve, dead layer thickness (t), Yafet-Kittel angle (θ_{YK}), magnetic moment (μ_B) of the sample NP3

Sample code	Crystallite size (nm)	Hc (Oe)	Ms (emu/g)	Mr (emu/g)	Mr/Ms	t (nm)	θ_{YK}	μ_B
NP3	28.6	162.05	42.35	6.74	0.159	0.73	24.71	1.77

The observed reduction in Ms in the NP3 may be explained on the basis of Neel's theory of ferrimagnetism. According to Neel's theory, three

International Journal of
Scientific Research in Science and Technology (IJSRST)
Print ISSN : 2395-6011, Online ISSN : 2395-602X
International Conference on Advanced Materials
Held on 14, 15 December 2017, Organized by Department of Physics,
St. Joseph's College, Trichy, Tamilnadu, India

kinds of exchange interaction exist in ferrites: interaction between magnetic ions in tetrahedral (A) and octahedral (B) sites (A-B interaction), interaction between the magnetic ions in octahedral (B) sites (B-B interaction) and interaction between the magnetic ions in tetrahedral (A) site (A-A interaction). But A-B interaction is very strong compared with A-A and B-B. According to Neel's theory magnetic moment per formula unit is given by,

$$\mu_{TH} = M_B - M_A \qquad (5)$$

where M_B and M_A represent the magnetic moment of ions in the octahedral and tetrahedral sites respectively. The net moments are determined according to the cations distribution estimated from the Rietveld refinement by assuming the magnetic moment of Fe^{3+} ion is 5 μ_B and that of Ni^{2+} ion is 1.7 μ_B. The total magnetic moments of ions present in the A site is much less than that of B site. This strengthens B-B interaction compared with A-B interaction and the collinear spin arrangement of B sub lattice gets disturbed. This suggests that canting angle is established and it can be explained by Yafet-Kittel sub lattice model [10][11]. According to Yafet-Kittel (Y-K) model, the canting angle (θ_{YK}) was calculated from the following equation,

$$\theta_{YK} = \frac{\cos^{-1}(M_A + \mu_B)}{M_B} \qquad (6)$$

where μ_B is the experimental magnetic moment per formula unit in Bohr magnetron (μ_B) of the sample and it is calculated from the equation,

$$\mu_B = \frac{Molecular\ weight \times M_s}{5585} \qquad (7)$$

The Y-K angles (θ_{YK}) are determined from the experimental magnetic moment (in Bohr magneton) estimated from the proposed cation distribution based on the Rietveld refinement. The estimated values of experimental magnetic moment (μ_B) and Yafet-Kittel (θ_{YK}) angle is given in the table 3. Y-K angles support the non-collinear spin structure in the B sub lattice and hence reduction in saturation magnetization value observed in the sample NP3.

3.6. Mossbauer Studies

Mossbauer spectra of the sample NP3 is shown in the figure 8. Mossbauer measurements were done at room temperature for exploring the magnetic nature prevailing at the cation sites. The Mossbauer spectrum was fit with NORMOS–SITE program and results obtained for the hyperfine parameters, which are the full width at half maxima (FWHM), isomer shift (IS), quadrupole splitting (QS) and the magnetic hyperfine field (BHF) are listed in the table 4. We could fit double sextet pattern in the room temperature spectrum, corresponding to Fe^{3+} ions at the A sites and B sites of the spinel structure, respectively. The hyperfine field calculated for the A and B sites are 48.9 T and 51.13T [12]. This is in good agreement with values reported for nano nickel ferrites in literature. Further, area under sextets pattern indicating Fe^{3+} ions in both sites equally contributing to the ferrimagnetic nature of the sample. Using fractional area of each sub spectrum, the Fe^{3+} ion ratio in both octahedral (B) and tetrahedral (A) site was calculated.The degree of inversion can be obtained from the equation

$$\frac{Area(A-site)}{Area(B-site)} = \frac{f_A}{f_B}\frac{x}{(2-x)} \qquad (8)$$

here $\frac{f_A}{f_B}$ is the ratio of the recoilless fractions equivalent to 0.94 at room temperature, x is the amount of Fe^{3+} ions present in the A-site and (2 – x) is the amount present in B-site. The estimated cations distribution for the samples is listed in table 4. It should be noted that the estimated cations distribution is well matches with that obtained from the Rietveld refined x-ray diffraction pattern (Table1).

International Journal of
Scientific Research in Science and Technology (IJSRST)
Print ISSN : 2395-6011, Online ISSN : 2395-602X
International Conference on Advanced Materials
Held on 14, 15 December 2017, Organized by Department of Physics,
St. Joseph's College, Trichy, Tamilnadu, India

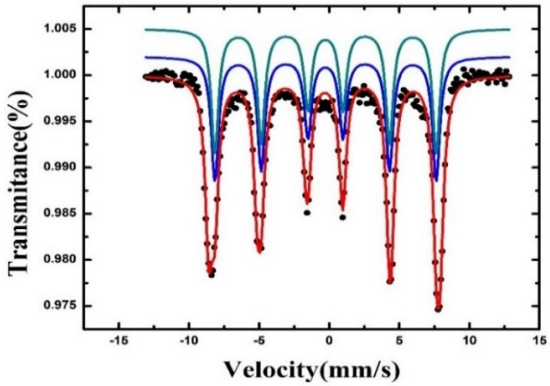

Figure 8. Mossbauer spectrum of the sample NP3

Table 4. Hyperfine parameters and cation distribution from Mossbauer spectra analysis of the sample NP3

	Site	FWHM Γ (mm/s)	Isomer Shift δ (mm/s)	quadrupole shift (mm/s)	Hyperfine field (Tesla)	% Area	Cation distribution
NP3	B-site	0.62	0.26	0.012	48.91	51.05	$[Ni_{0.89}Fe_{1.11}]^{B}O_4$
	A-site	0.62	0.35	0.023	51.13	48.95	$(Ni_{0.11}Fe_{0.89})^{A}$

4. Conclusion

Nickel ferrite nano-powders were successfully synthesized by a simple spray pyrolysis method – a low cost, low temperature high yield process. The effects of annealing on the structural properties of the samples are studied by XRD. The crystallite size of the samples increases with annealing. HRTEM micrograph confirmed ultrafine particles with cubic shape. Two strong absorption bands at v_1 and v_2 in the FTIR spectrum confirm spinel structure of the sample. The weak band at the tetrahedral site in the FTIR spectrum shows the mixed spinel structure of nickel ferrite nanoparticles. The magnetic parameters, determined from room temperature VSM, are in conformity with that of soft ferrimagnetic nature of the prepared sample. The same has been confirmed from room temperature Mossbauer studies of the sample. Further, the cation distribution obtained from the Mossbauer studies matches well with that obtained from theRietveld refinement of XDR pattern, thereby confirming the mixed spinel structure in the nickel ferrite nanoparticles.

References

[1] Y. Yang et al., "Synthesis of nonstoichiometric zinc ferrite nanoparticles with extraordinary room temperature magnetism and their diverse applications," J. Mater. Chem. C, vol. 1, no. 16, p. 2875, 2013.

[2] Z. Karcıoğlu Karakaş, R. Boncukcuoğlu, İ.H. Karakaş, and M. Ertuğrul, "The effects of heat treatment on the synthesis of nickel ferrite ($NiFe_2O_4$) nanoparticles using the microwave assisted combustion method," J. Magn. Magn. Mater., vol. 374, pp. 298–306, 2015.

[3] X. Lasheras et al., Chemical Synthesis and

Magnetic Properties of Monodisperse Nickel Ferrite Nanoparticles for Biomedical Applications, vol. 120, no. 6. 2016.

[4] A. Jafari, S. Farjami Shayesteh, M. Salouti, and K. Boustani, "Effect of annealing temperature on magnetic phase transition in Fe_3O_4 nanoparticles," J. Magn. Magn. Mater., vol. 379, no. December, pp. 305–312, 2015.

[5] L. Kumar, P. Kumar, and M. Kar, "Cation distribution by Rietveld technique and magnetocrystalline anisotropy of Zn substituted nanocrystalline cobalt ferrite," J. Alloys Compd., vol. 551, no. February, pp. 72–81, 2013.

[6] R.D. WALDRON, "Infrared spectra of Ferrites," Phys. Rev., vol. 99, no. 6, pp. 1727–1734, 1955.

[7] S.A. Mazen, "Tetravalent ions substitution in Cu-ferrite; structure formation and electrical properties," Mater. Chem. Phys., vol. 62, no. 2, pp. 131–138, 2000.

[8] S. Maensiri, C. Masingboon, B. Boonchom, and S. Seraphin, "A simple route to synthesize nickel ferrite (NiFe2O4) nanoparticles using egg white," Scr. Mater., vol. 56, no. 9, pp. 797–800, 2007.

[9] J. Chen, C. Sorensen, K. Klabunde, G. Hadjipanayis, E. Devlin, and A. Kostikas, "Size-dependent magnetic properties of $MnFe_2O_4$ fine particles synthesized by coprecipitation," Phys. Rev. B, vol. 54, no. 13, pp. 9288–9296, 1996.

[10] H.M. El-Sayed, I.A. Ali, A. Azzam, and A.A. Sattar, "Influence of the magnetic dead layer thickness of Mg-Zn ferrites nanoparticle on their magnetic properties," J. Magn. Magn. Mater., vol. 424, pp. 226–232, 2017.

[11] Y. Yafet and C. Kittel, "Antiferromagnetic Arrangements in Ferrites," Phys. Rev., vol. 87, no. 2, pp. 290–294, 1952.

[12] V. Šepelák et al., "Nanocrystalline nickel ferrite, $NiFe_2O_4$: Mechanosynthesis, nonequilibrium cation distribution, canted spin arrangement, and magnetic behavior," J. Phys. Chem. C, vol. 111, no. 13, pp. 5026–5033, 2007.